



Function of the pseudo phosphotransfer proteins has diverged between rice and Arabidopsis

John Vaughan-Hirsch^{1,†,‡}, Emily J. Tallerday^{2,‡,*} , Christian A. Burr^{2,‡}, Charlie Hodgens², Samantha L. Boeshore², Kevin Beaver², Allison Melling², Kartika Sari^{1,3}, Ian D. Kerr⁴, Jan Šimura⁵, Karin Ljung⁵, Dawei Xu⁶, Wanqi Liang⁶, Rahul Bhosale^{1,7}, G. Eric Schaller⁸, Anthony Bishopp^{1,*} and Joseph J. Kieber^{2,*} 

¹School of Biosciences, University of Nottingham, Loughborough LE12 5RD, UK,

²Department of Biology, University of North Carolina, Chapel Hill, NC 27599, USA,

³FKIP, Universitas Muhammadiyah Metro, Lampung 34111, Indonesia,

⁴University of Nottingham, Loughborough NG7 2UH, UK,

⁵Umeå Plant Science Centre, Department of Forest Genetics and Plant Physiology, Swedish University of Agricultural Sciences (SLU), Umeå 901 83, Sweden,

⁶School of Life Science and Biotechnology, Shanghai Jiao Tong University, Shanghai, China,

⁷Future Food Beacon of Excellence and School of Biosciences, University of Nottingham, LE12 5RD, UK, and

⁸Department of Biological Sciences, Dartmouth College, Hanover, NH 03755, USA

Received 13 December 2019; revised 4 January 2021; accepted 5 January 2021.

*For correspondence (e-mail anthony.bishopp@nottingham.ac.uk; jkieber@bio.unc.edu).

‡These authors contributed equally.

†Present address: Department of Biosystems, University of Leuven, Leuven, 3001, Belgium

‡Present address: Department of Plant Biology, Michigan State University, East Lansing, MI, 48823, USA

SUMMARY

The phytohormone cytokinin plays a significant role in nearly all aspects of plant growth and development. Cytokinin signaling has primarily been studied in the dicot model Arabidopsis, with relatively little work done in monocots, which include rice (*Oryza sativa*) and other cereals of agronomic importance. The cytokinin signaling pathway is a phosphorelay comprised of the histidine kinase receptors, the authentic histidine phosphotransfer proteins (AHPs) and type-B response regulators (RRs). Two negative regulators of cytokinin signaling have been identified: the type-A RRs, which are cytokinin primary response genes, and the pseudo histidine phosphotransfer proteins (PHPs), which lack the His residue required for phosphorelay. Here, we describe the role of the rice PHP genes. Phylogenetic analysis indicates that the PHPs are generally first found in the genomes of gymnosperms and that they arose independently in monocots and dicots. Consistent with this, the three rice PHPs fail to complement an Arabidopsis *php* mutant (*aphp1/ahp6*). Disruption of the three rice PHPs results in a molecular phenotype consistent with these elements acting as negative regulators of cytokinin signaling, including the induction of a number of type-A RR and cytokinin oxidase genes. The triple *php* mutant affects multiple aspects of rice growth and development, including shoot morphology, panicle architecture, and seed fill. In contrast to Arabidopsis, disruption of the rice PHPs does not affect root vascular patterning, suggesting that while many aspects of key signaling networks are conserved between monocots and dicots, the roles of at least some cytokinin signaling elements are distinct.

Keywords: *Oryza sativa*, plant hormones, cytokinin, two-component signaling.

INTRODUCTION

Cytokinins are N⁶-substituted adenine derivatives that regulate diverse aspects of plant growth and development (Mok and Mok, 2001; Hwang *et al.*, 2012; Kieber and Schaller, 2014; Schaller *et al.*, 2015; Kieber and Schaller, 2018b; Wybouw and Rybel, 2019), including a key role in regulating seed yield and root architecture (Jameson and Song,

2016). The cytokinin signaling pathway in plants is similar to bacterial and yeast two-component signal transduction pathways, specifically to the His-Asp multi-step phosphorelays that are comprised of sensor histidine (His) kinases (HKs), authentic His phosphotransfer proteins (AHPs) and response regulators (RRs) (Hwang *et al.*, 2012; Schaller *et al.*, 2015; Kieber and Schaller, 2018a). The cytokinin

signaling elements in rice, Arabidopsis and other plants are encoded by small gene families (Pareek *et al.*, 2006; Du *et al.*, 2007; Schaller *et al.*, 2007; Pils and Heyl, 2009; Tsai *et al.*, 2012) whose members have overlapping functions in Arabidopsis (Higuchi *et al.*, 2004; Nishimura *et al.*, 2004; To *et al.*, 2004; Hutchison and Kieber, 2007; Argyros *et al.*, 2008). Rice has four HK cytokinin receptors that, similar to their maize and Arabidopsis counterparts, likely bind to various cytokinin species with distinct affinities (Romanov *et al.*, 2006; Lomin *et al.*, 2011; Stolz *et al.*, 2011). The AHPs are the direct targets of the HK receptors and act as intermediates in the transfer of a phosphate from the HKs to the downstream RRs (Suzuki *et al.*, 1998; Tanaka *et al.*, 2004; Hutchison *et al.*, 2006). The RRs fall into two main classes called type-A and type-B RRs. In both classes, an N-terminal receiver domain harbors an Asp residue that is the target of phosphotransfer. Type-B RRs mediate the transcriptional response to cytokinin; type-A RRs lack a DNA-binding output domain, are rapidly and specifically induced by cytokinin, and function as negative feedback regulators in cytokinin signaling (Brandstatter and Kieber, 1998; D'Agostino *et al.*, 2000; To *et al.*, 2004; Jain *et al.*, 2006; Tsai *et al.*, 2012).

The canonical cytokinin signaling pathway is inhibited by two sets of signaling elements; the aforementioned type-A RRs (To *et al.*, 2004) and in Arabidopsis, the pseudo phosphotransfer protein AHP1/AHP6 (hereafter referred to simply as AHP6), in which the conserved His at the phospho-receiving site is replaced with an Asn residue (Suzuki *et al.*, 2000; Mähönen *et al.*, 2006). AHP6 is induced by auxin and modulates the interaction between these two hormones to regulate key developmental processes, such as root vascular patterning, the formation of passage cells, lateral root organogenesis, proliferation of the inflorescence meristem, shoot phyllotaxy and gynoecium development (Mähönen *et al.*, 2006; Bartrina *et al.*, 2011; Moreira *et al.*, 2013; Besnard *et al.*, 2014; Müller *et al.*, 2017;

Andersen *et al.*, 2018). While PHP function has been analyzed in Arabidopsis, nothing is known regarding PHP function in monocots, including rice.

Rice is a model for investigating cytokinin function in monocots, with genetic studies linking cytokinin metabolism to inflorescence development (Ashikari *et al.*, 2005; Kurakawa *et al.*, 2007; Gu *et al.*, 2015; Yeh *et al.*, 2015). Furthermore, several studies have shed light on cytokinin signaling in rice, including HK receptors (Ding *et al.*, 2017; Burr *et al.*, 2020), type-B RRs (Worthen *et al.*, 2019), and type-A RRs (Hirose *et al.*, 2007; Wang *et al.*, 2019). Here, we examined the role of the genes encoding rice pseudo His phosphotransfer (PHP) proteins. Our analysis indicates that, similar to the Arabidopsis AHP6 protein, the rice PHPs are negative regulators of cytokinin signaling, although they appear to have arisen independently of their dicot counterparts. Consistent with their independent origins, the rice PHPs fail to complement an Arabidopsis *ahp6* mutant and disruption of the PHPs in rice results in a subset of phenotypes distinct from the cognate Arabidopsis mutant, suggesting that monocot and dicot PHPs play distinct roles in regulating growth and development.

RESULTS

Phylogenetic analysis of phosphotransfer proteins in plants

We analyzed available plant sequences for His phosphotransfer proteins (HPs), both AHPs and PHPs, respectively (Schaller *et al.*, 2007). AHPs were found in all plant species examined, including algae. While PHPs are present in early diverging angiosperms, including *Peperomia obtusifolia* and *Amborella trichopoda*, and in gymnosperms (*Picea abies* and *Pinus taeda*), they were not found in bryophytes (*Selaginella moellendorffii*, *Physcomitrella patens*, *Sphagnum* and *Marchantia polymorpha*) (Figure 1a; Figures S1 and S2; Tables S1 and S2). To explore the evolutionary

Figure 1. Rice histidine (His) phosphotransfer proteins (HPs).

(a) Phylogenetic tree of HPs from selected lineages: *Arabidopsis thaliana* (At, brown), *Oryza sativa* (Os, purple), *Zea mays* (Zm, pink), *Picea abies* (Pa, green), *Physcomitrella patens* (Pp, blue) and *Saccharomyces cerevisiae* (Sc, black). See Table S1. Scale bar represents diverged distance. Branch support values for the phylogenetic reconstruction are displayed as a percentage on each branch. Vertical orange bar indicates the pseudo His phosphotransfer proteins (PHPs), which are also indicated with an *.

(b) Abbreviated multiple sequence alignment for the proteins shown in (a), with the numbers indicating the position of the first amino acid depicted. The position of the conserved His residue that is the target of phosphorylation found in all authentic His phosphotransfer proteins (AHPs) is indicated with a red arrow at the bottom.

(c) Phosphotransfer assays using yeast SLN1 HK and Rec domains with various rice phosphotransfer proteins. Purified proteins were incubated with γ -³²P ATP as described in methods in a kinase assay. Reactions were analyzed by sodium dodecyl sulfate–polyacrylamide gel electrophoresis followed by imaging using a phosphor screen. Lanes contained the indicated purified proteins. PHP1, PHP2 or PHP3 in the last three lanes are indicated by the red numbers. Owing to the fact that bead band protein was used, not all lanes have been loaded evenly, and consequently bands appear faint in some lanes (e.g., lane 6).

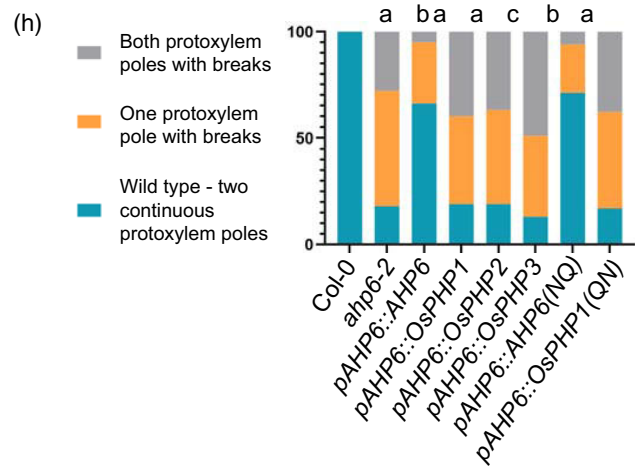
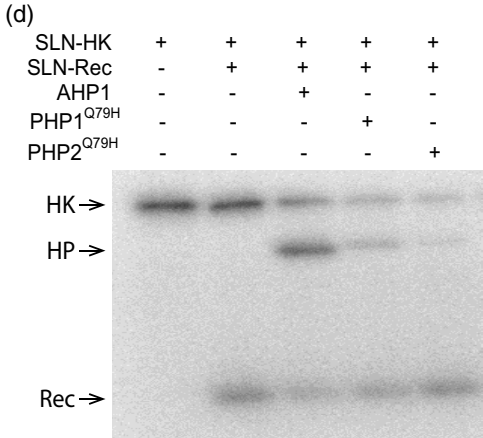
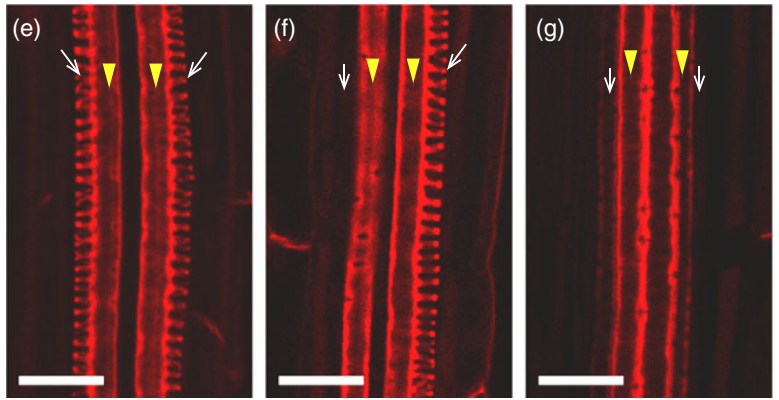
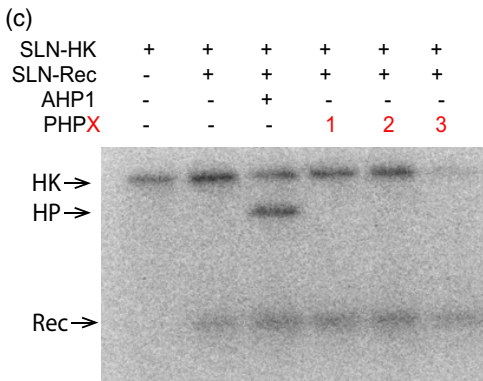
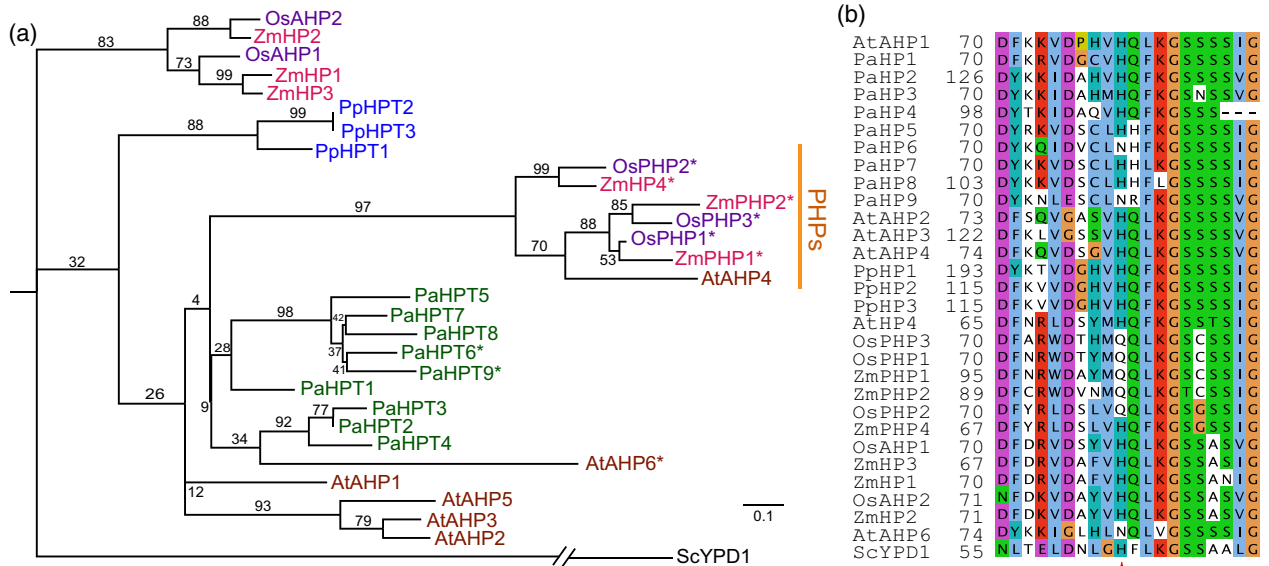
(d) Phosphotransfer assays with rice PHPs in which the receiving site is substituted from a Gln substituted for His. *In vitro* kinase assays were performed as in (c). Lanes contained the indicated purified proteins.

(e,f,g) Functional analysis of rice PHPs in Arabidopsis. Arrows indicate protoxylem and yellow arrowheads metaxylem. Absence of protoxylem is indicated with white arrowheads. The three main phenotypic classes are shown: E, wild-type pattern; F, the class with a break in one protoxylem pole; and G, the stronger class with breaks in two protoxylem poles.

(h) Quantification of phenotypic classes in various Arabidopsis lines. At least three independent transgenic lines were assayed for each construct, with at least 20 individuals per line. Pearson chi-squared tests shows that only pAHP6::AHP6 and pAHP6::AHP6 (NQ) differ significantly from the *ahp6-2* control ($P \leq 0.0001$).

history of this gene family better, we created a rooted maximum-likelihood tree with predicted HPs from 48 plant species with available full genome sequences and one species

for which a transcriptome assembly was available. Two major PHP clades are found, one from dicots that contain an Asn at the position of the conserved His residue in HPs,



and one from monocots that contains a Gln at this position (Figure 1a,b; Figures S1 and S2). Based on this phylogeny, the rice PHPs and the Arabidopsis AHP6 proteins are likely not orthologous, as the most parsimonious solutions suggest that their common ancestral protein most likely predates the split between the AHPs and PHPs. This suggests that there have been at least two evolutionary events that led to the formation of PHPs; one event giving rise to a PHP(Asn) class as seen in eudicots and a second giving rise to a PHP(Gln) class seen in monocots. The gymnosperm PHPs identified have an Asn at this position, similar to dicots. Additionally, the PHP gene family appears to have expanded in the monocot lineage compared with the dicots. For example, whereas most dicots have one or two PHPs (e.g., Arabidopsis has a single PHP, AHP6, and *Medicago truncatula* has two PHPs; Tan *et al.*, 2019), rice has three and maize has two. Interestingly, the Arabidopsis AHP4 protein groups with the monocot PHP clade (Figure 1a). Consistent with this, genetic analysis indicated that AHP4 plays a negative role in various cytokinin responses (Hutchison *et al.*, 2006), suggesting that despite the presence of a His at the canonical phosphorylation site, some predicted HPs may act as PHPs.

Rice PHPs do not function in a phosphorelay *in vitro*

We examined if the rice PHPs could participate as positive components in the phosphorelay. Rice PHP proteins were expressed and purified from insect cells and their activity was analyzed using an *in vitro* phosphotransfer assay using the yeast SLN1 HK and receiver domains (Ault *et al.*, 2002a; Janiak-Spens *et al.*, 2005) together with AHP1 from rice (Figure 1c,d). This assay has been used previously to show transfer of a ^{32}P γ -labeled ATP phosphoryl group from the conserved His residue of SLN1-HisK to a conserved Asp residue within the SLN1-Rec, and subsequently to a conserved His residue within a plant AHP protein (Posas *et al.*, 1996; Mähönen *et al.*, 2006). In reactions containing AHP1, phosphate were transferred from SLN1-HisK to SLN1-Rec and on to AHP1. However, when PHP1, 2 or 3 were substituted for AHP1, no phosphotransfer was observed to the PHPs (Figure 1c). In similar reactions in which we replaced the Gln with a His at the phospho-receiving site, the ^{32}P -labeled ATP was transferred on to PHP1^{Q79H} and PHP2^{Q79H}, albeit at a lower level than AHP1 (Figure 1d). Collectively these results suggest that similar to Arabidopsis, the rice PHPs do not function as phosphotransfer proteins.

We exploited the loss-of-protaxylem phenotype observed in the Arabidopsis *ahp6* mutant to test if the rice PHPs could functionally substitute for this Arabidopsis PHP. Similar to previous observations (Mähönen *et al.*, 2006), the *ahp6-2* mutants displayed an incompletely penetrant phenotype in which protaxylem was missing in patches along the root; whereas wild-type plants invariably

had two xylem poles (Figure 1e), protoxylem failed to differentiate in either one or two poles in *ahp6* (Figure 1f,g). We have previously been able to complement fully the *ahp6* with a genomic AHP6 transgene (Mähönen *et al.*, 2006); however, a transgene expressing the AHP6 coding sequence (CDS) from a 1.6-kb promoter (pAHP6:AHP6) resulted in significant, albeit only partial complementation of *ahp6-2*. Expression of a mutant version of this construct in which Asn⁸³ of AHP6 (at the site of the canonical His target in AHP1-5) was replaced with a Gln (pAHP6:AHP6^{N83Q}) resulted in the partial rescue of the *ahp6* mutant phenotype, which was indistinguishable from pAHP6:AHP6 (Figure 1h). This indicates that either Asn or Gln at the phospho-receiving site is sufficient for AHP6 function in vascular development. When expressed using this same segment of the AHP6 promoter, all three rice PHPs were unable to rescue the *ahp6-2* mutants. This was not dependent on the identity of the amino acid at the phospho-receiving site, as replacing Gln79 with Asn in rice PHP1 did not change its ability to complement *ahp6* (Figure 1h). Given the phylogenetic distance separating the monocot and dicot PHPs, it is likely that divergence in other residues has led to components of the rice and Arabidopsis two-component signaling machinery being unable to interact functionally *in planta*.

Role of the PHPs in rice growth and development

To investigate potential roles for the PHPs in rice, we examined their expression patterns. To this end, we fused a GUS reporter gene to 3 kb of sequence upstream of the translational start from each PHP and examined the expression patterns of the reporter in 14-day-old transgenic seedlings. All the PHP reporters were expressed in the root tip and root hairs (Figure 2a,b,h,i,o,p). PHP1 was expressed broadly in the root tip within the vascular cylinder and the inner cortex (Figure 2a,c), and at the base of lateral root primordia. PHP2 and PHP3 were detected specifically in the epidermis, with PHP2 expression being restricted to root hair cells (Figure 2i,j,p,q). All three PHPs were expressed abundantly in leaves, with the highest expression in stomata (Figure 2d,k,r). In panicles, PHP2 and PHP3 were strongly expressed, while we only saw transient expression of PHP1 in a few spikelets (Figure 2e,l,s). PHP1 appears to be localized to developing embryos (Figure 2f,g), whereas PHP2 and PHP3 show cell-type specific patterns within the lemma and palea (Figure 2m,n,t,u). These PHP expression patterns are generally consistent with the analysis of PHP transcript levels obtained from tissue-specific microarray and RNA-sequencing (RNA-Seq) datasets (Figure S3) (Sato *et al.*, 2011; Xia *et al.*, 2017).

To define the role of the PHPs in rice growth and development further, we created single and multiple *php* mutant lines using CRISPR/Cas9. We identified rice lines mutated

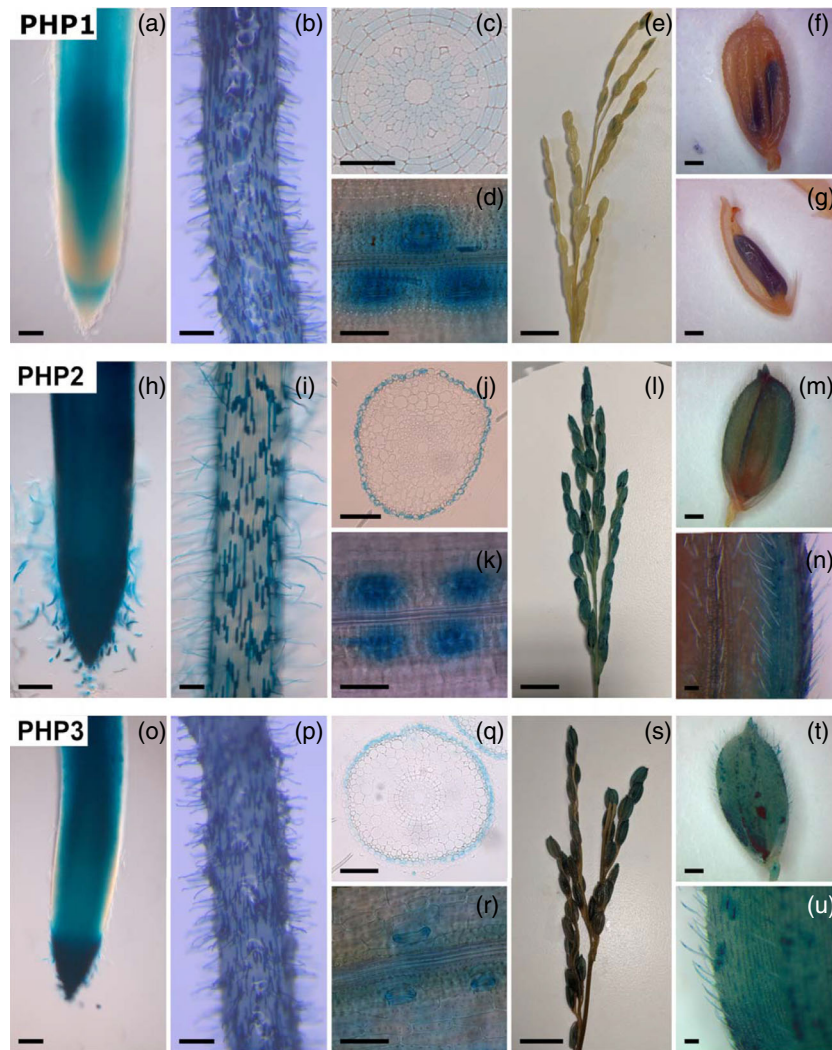


Figure 2. Expression pattern of pseudo histidine phosphotransfer proteins (PHPs) in rice.

GUS staining showing expression of the transcriptional reporters in stable rice transformants.

(a–g) Expression of PHP1::GUS; (h–n) Expression of PHP2::GUS; (o–u) Expression of PHP3::GUS. (a) PHP1::GUS signal can be observed broadly throughout the root tip and (b) in the sclerenchyma and exodermis in the basal zone of primary root and root hairs. (c) Cross-sections taken from the root apex reveal staining in the procambial cells, with the highest levels in the cells closest to the central xylem element, and in the inner cortex layer. (d,k,r) For all three PHP reporters, staining is seen in the first leaves and is associated with stomata. (e) PHP1::GUS signal is low in inflorescences and (f,g) is localized to developing embryos only. (h) PHP2::GUS shows staining in the whole of the primary root tip and (i) signal is present in root hair cells in more basal zones of the primary root. (j) Cross-sections from the root apex show signal localized to sclerenchyma and exodermis. (l,m,n) PHP2::GUS signal is seen widely throughout whole inflorescences and in spikelets is localized to the corner regions of lemma and palea epidermis. PHP3::GUS signal can be seen throughout the (o) root tip and (p) root hairs. (q) Cross-sections from the basal zone of the primary root show expression in the sclerenchyma and exodermis. (s) PHP3::GUS signal is seen strongly throughout the inflorescence, and (t,u) mainly localized to the narrow cell files on either side of the globular cells of the epidermal layer of the lemma and palea. At least two independent transgenic lines for each reporter were used and representative images taken. Scale bars: (a,b,h,i,j,n,o,p,q,r,u) 100 μ m; (c,d,k,r) 50 μ m; (e,l,s) 10 mm; (f,g,m,t) 1 mm.

for each *PHP* gene; *php1-1* has a 4-bp deletion in its second exon; *php2-1* and *php3-1* both have 1-bp insertions in their second exons (Figure 3a,b). We also created a *php1,2,3* triple mutant. Initially, we examined processes in which AHP6 is known to play a role in Arabidopsis, (Mähönen *et al.*, 2006) and found no associated phenotypes. We compared root sections of wild-type and the *php* triple mutant and observed no changes in vascular patterning or root

anatomy (Figure 3c; Figure S4). Equally, we did not observe any differences in root architecture in plants grown on agar plates. We observed no significant changes in root number, root lengths, or root system area convex hull (Figure S5). Surprisingly, although *PHP2* (and to a lesser extent *PHP3*) appears to be specifically expressed within root hairs, under our conditions we did not see a difference in either root hair length or density (Figure S5).

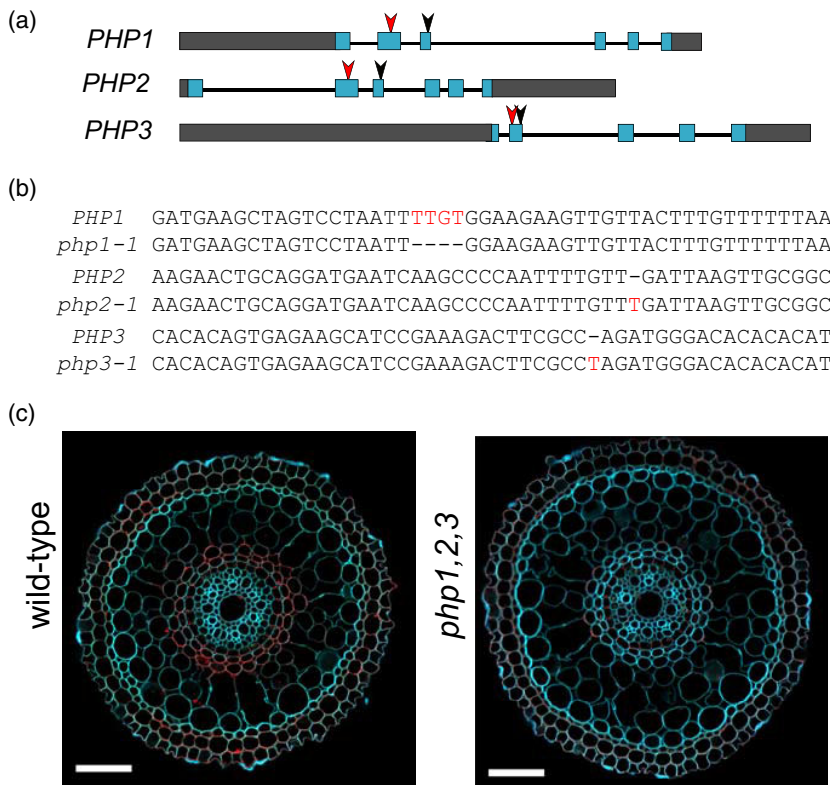


Figure 3. Analysis of pseudo histidine phospho-transfer protein (PHP) function.

(a) Gene diagrams for *PHP1*, *PHP2* and *PHP3*. Gray boxes denote untranslated regions, lines are introns and blue boxes are exons. Red arrows denote the CRISPR/Cas9 target site, and black arrows the location of where the conserved histidine residue would be.

(b) Mutations in the *php* mutant lines created using CRISPR/Cas9. Insertions are indicated by dashed lines in the wild-type sequence (top), deletions are shown with dashes in the mutant sequence (bottom). Red indicates deleted nucleotides.

(c) Radial cross-section of wild-type and *php1,2,3* roots. Note that no apparent differences are seen in vascular anatomy. At least nine plants per genotype were sectioned 5 cm above the root tip. Scale = 50 μm .

Moving our attention to the shoot, while the lower order mutants were generally comparable with the wild type, the triple mutant consistently displayed substantial alterations in various aspects of shoot and inflorescence morphology and architecture that had not been reported in *ahp6* mutants (Figure 4a,b). The overall stem height of the triple mutant was significantly shorter than the wild type (Figure 4c); however, the length and width of leaves (Figure 4d,e) and the number of panicles (Figure 4f) were comparable between the *php1,2,3* mutant and the wild type. Previous studies have shown that altered cytokinin levels could have profound effects on panicle development in rice (Ashikari *et al.*, 2005; Kurakawa *et al.*, 2007; Gu *et al.*, 2015; Yeh *et al.*, 2015). Consistent with this, the triple mutant panicles show multiple alterations as compared with the wild type, including overall smaller size with fewer primary and secondary branches (Figure 4g–j). Fewer spikelets per panicle were seen in the triple mutant, with overall fewer filled seed per panicle as compared with wild type (Figure 4h,k), although the seeds were of comparable weight (Figure 4l). Profiling of cytokinin levels within spikelets revealed that cytokinin levels were altered in the *php* mutants, with a small but statistically significant decrease in the concentration of both *cis*- and *trans*-zeatin and an increase in the levels of dihydrozeatin and isopentyl adenine (Table S3). There did not appear to be any substantial effects on leaf phyllotaxy in the triple mutant.

Molecular analysis of the *php* triple mutants suggests that they act as negative regulators of cytokinin signaling

We assayed the response of the *php* triple mutant to cytokinin using growth assays of 7-day-old rice seedlings grown on an agar medium. Growth of wild-type seedlings in increasing concentrations of the cytokinin 6-benzylaminopurine (BA) caused a decrease in root and shoot growth, as well as a reduction in the number of crown roots (Figure S6). The response of the triple *php* mutant was comparable with the wild type in all aspects of this growth assay (Figure S6), suggesting that disruption of the PHPs does not affect the response to exogenous cytokinin, at least in these assays.

To examine the molecular response of the mutant to cytokinin, we used RNA-Seq to measure the effect of a 2-h treatment with cytokinin (0, 100 nM and 5 μM BA) on the transcriptome of wild-type and *php* triple mutant roots from hydroponically grown plants in sterile culture with constant air flow to promote transpiration. In total, 793 and 1292 genes were induced (false discovery rate [FDR] ≤ 0.05 and fold-change [FC] ≥ 1.5) in wild-type roots in response to 100 nM and 5 μM BA, respectively, under these conditions (Figure 5c and Table S4). Most of the genes (84.5%) induced in response to 100 nM BA were also induced at the higher concentration of BA. Conversely, many (48%) of the genes induced at 5 μM BA in wild-type roots were not induced at the lower BA concentration. Similar to previous

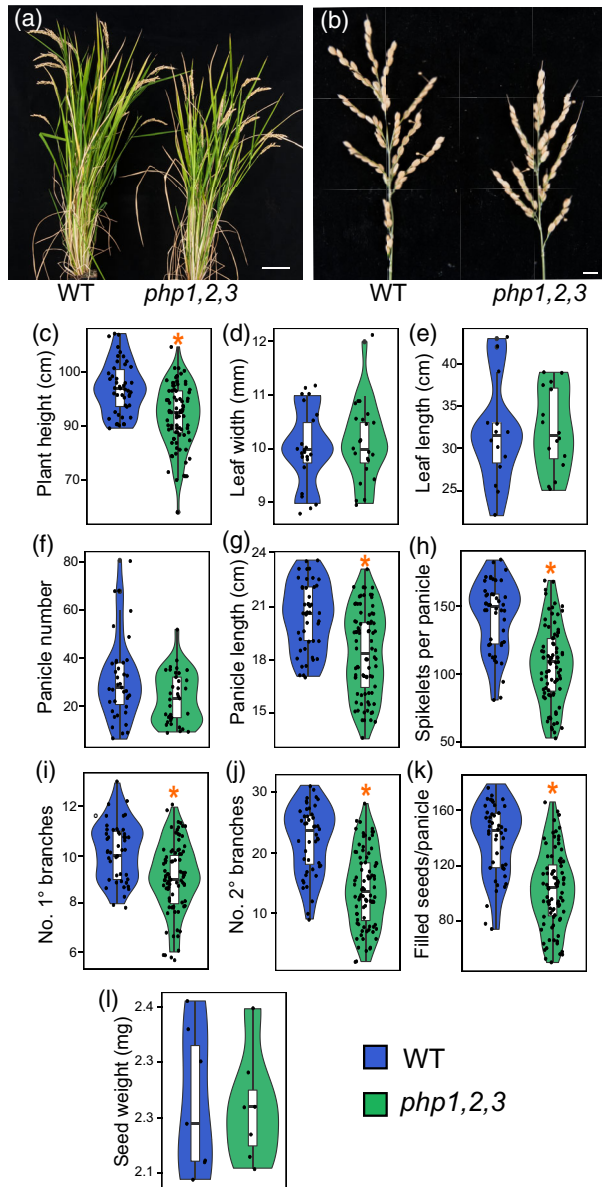


Figure 4. Shoot and panicle morphology of the *php1,2,3* triple mutant. (a) Representative images of 19-week-old wild-type (WT) and *php1,2,3* plants. Scale = 10 cm. (b) Representative images of mature, dried panicles from WT and *php1,2,3* plants. Scale = 1 cm. (c–g) Quantification of (c) plant height ($n \geq 49$), (d) leaf width ($n \geq 23$), (e) flag leaf length ($n \geq 14$), (f) panicle number ($n \geq 11$) and (g) panicle length ($n \geq 44$) from WT and *php1,2,3* triple mutant plants grown in soil as described in Experimental procedures. (h–k) Quantification of various aspects of panicles in WT and *php1,2,3* triple mutant plants: (h) spikelets per panicle; (i) number of primary branches per panicle; (j) number of secondary branches per panicle; (k) number of filled seed per panicle; (h–k) $n \geq 46$. (l) Quantification of the weight of 100 seeds from WT and *php1,2,3* triple mutant. Seeds of approximately equal age were de-hulled and 100 seeds were counted manually and weighed. g/100 seeds ($n = 7$). Data for (c–l): *statistical significance determined by a Student's *t*-test with $P < 0.01$.

transcriptome studies (Raines *et al.*, 2016), fewer genes were identified as downregulated in response to cytokinin in wild-type rice roots in these conditions (490 and 867 at 100 nM and 5 μ M, respectively; FDR ≤ 0.05 and FC ≤ 0.66) (Figure 5d and Table S4). Similar to the induced genes, most of the genes downregulated in response to 100 nM BA, were also downregulated in response to 5 μ M BA in wild-type roots, but only approximately half of the genes downregulated in response to 5 μ M BA were downregulated at the lower BA concentration. Overall, these data suggest that numerous genes are regulated by cytokinin specifically at elevated concentrations.

To explore the role of the PHPs, we examined the expression of the type-A RRs, which are well characterized cytokinin primary response genes (Brandstatter and Kieber, 1998). In the absence of exogenous cytokinin, expression of multiple type-A RRs (*RR2*, *RR4*, *RR6*, *RR9*, and *RR10*) was elevated in the *php* triple mutant roots as compared with the wild type (Figure 5a), consistent with an upregulation of cytokinin signaling in the mutant. The seven other type-A RRs were expressed at very low or undetectable levels in rice roots. The level of expression of type-A RRs was elevated in response to both doses of BA in wild-type roots (Figure S7), consistent with previous studies (Tsai *et al.*, 2012). In the presence of both doses of cytokinin, the levels of type-A RR transcripts were comparable in wild-type and triple mutant roots (Figure S7), indicating that the PHPs do not affect type-ARR gene expression at the elevated cytokinin levels that result from exogenous application of BA. We examined the expression of other genes involved in cytokinin signaling (*HKs*, *AHPs*, and type-B RRs) and metabolism (*IPTs*, *LOGs*, *CKXs*, and *cZOG1*) (Table S5). There was a strong induction (>20-fold induced) in *php1,2,3* of a putative *cis*-zeatin *O*-glucosyltransferase 1 gene (Os04g0565200), which likely encodes an enzyme that glycosylates cytokinin to inactivate it (Kudo *et al.*, 2012). A subset of the *CKX* genes (*CKX1*, *CKX3*, and *CKX4*), which encode cytokinin oxidases that degrade cytokinin, were differentially expressed in the *php* triple mutant (Figure S7). For all three of these *CKX* genes, the expression was elevated in the absence of exogenous cytokinin as compared with the wild type. For *CKX3*, there was also an increased level of expression in the mutant at 5 μ M BA. Thus, negative regulators of both cytokinin signaling (type-A RRs) and cytokinin levels (*CKX*) are upregulated in the *php* triple mutants in the absence of exogenous cytokinin, suggesting a potential feedback of these mutations on cytokinin homeostasis.

We next examined the global effects of the *php* mutant on transcription. In the absence of exogenous cytokinin, 397 genes were upregulated and 122 downregulated in the *php* triple mutant as compared with wild-type roots (FDR ≤ 0.05 and FC ≥ 1.5 or FC ≤ 0.66) (Table S6). Gene Ontology

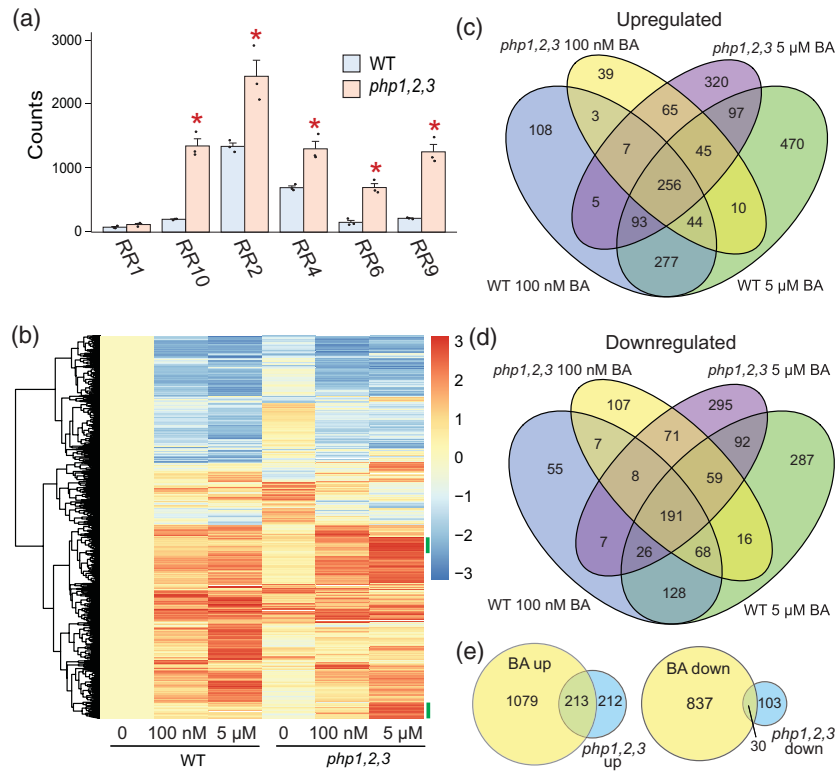


Figure 5. RNA-sequencing analysis of *php* mutants.

(a) Normalized expression values for a subset of the type-A response regulators (RRs) in the absence of exogenous cytokinin. Type-A RR genes with very low expression values (<50 normalized reads in all samples) were excluded. Values represent the mean ($n = 3$) \pm SE. Asterisks indicate statistical significance determined by DESeq2 for the wild type (WT) versus *php1,2,3* condition in the untreated condition. Significance was defined as having an adjusted P -value lower than 0.05, with P -value adjustments performed using a weighted Benjamini-Hochberg procedure.

(b) Heatmap of all genes that are differentially expressed after 2 h treatment with 6-benzylaminopurine (BA) (WT or *php1,2,3* control plants compared with 100 nM BA- or 5 μM BA-treated plants). Genes are scaled within rows with the WT untreated plants as the reference. Scale is indicated to the right with red bars indicating upregulation relative to untreated WT plants and blue bars downregulated genes. Green bars to the right of the heatmap indicate genes hyperinduced in response to cytokinin in the *php1,2,3* mutant. Bar units are standard deviations are relative to untreated WT.

(c,d) Gene set overlap between genes upregulated (false discovery rate [FDR] \leq 0.05 and fold-change [FC] \geq 1.5) (c) or downregulated (FDR \leq 0.05 and FC \leq 0.66) (d) after treatment with BA in the WT and *php1,2,3* mutants after treatment with 100 nM BA or 5 μM BA.

(e) Gene set overlap between genes differentially expressed in WT by treatment with 100 nM BA and genes differentially expressed between the WT and *php1,2,3* mutant with no BA treatment (FDR \leq 0.05 and FC \geq 1.5 or FC \leq 0.66).

enrichment using g:Profiler (Raudvere *et al.*, 2019) identified DNA-binding transcription factor activity, transcription regulator activity, and DNA binding to be the most significantly enriched terms, suggesting that the *PHP* loci affect multiple downstream regulatory networks (Table S7). Cytokinin dehydrogenase activity was also significantly enriched (adjusted P -value 0.0078). Enrichment analysis for biological processes showed high enrichment of processes associated with amino acid or amine transport alongside cytokinin signaling and RNA regulation (Table S7). Kyoto Encyclopedia of Genes and Genomes (KEGG) pathway enrichment analysis showed the greatest enrichment in plant hormone signal transduction and zeatin biosynthesis (Table S7). Collectively, these results show a strong overlap with processes previously associated with cytokinin, but also highlight some potential roles in amino acid transport. We examined if the genes differentially expressed in

the mutant were significantly enriched for cytokinin-responsive genes. Indeed, 50% of the genes upregulated in the *php* triple mutant overlapped with genes induced by cytokinin in the wild-type roots ($P(X \geq 213) = 3.5 \times 10^{-156}$, hypergeometric test) and 23% of the genes downregulated in the mutant overlapped with genes repressed in wild-type roots in response to exogenous cytokinin ($P(X \geq 30) = 5.8 \times 10^{-16}$, hypergeometric test) (Figure 5e). In contrast, there was nearly no overlap between genes upregulated in the *php* mutant and downregulated by cytokinin in wild-type roots (two of 397), nor in genes downregulated in the mutant and upregulated by cytokinin (two of 122). Together, these results show that a significant number of genes affected by the PHPs are downstream of cytokinin response. This is consistent with the PHPs acting as negative regulators of cytokinin signaling in roots, similar to the proposed role of the *AHP6* gene in *Arabidopsis*.

While it is feasible that these proteins may have some function independent of cytokinin, it is clear that a sizeable number of genes affected in these mutants are directly related to the cytokinin response.

While the effects of the *php* mutations on gene expression indicate a redundant role as negative regulators of endogenous cytokinin signaling, the effects in response to exogenous cytokinin are less clear. A set of genes that are hyperregulated in response to cytokinin in the *php* triple mutant as compared with the wild type (Figure 5b; green vertical bars), are consistent with a role as negative regulators of cytokinin signaling. However, in addition, a set of genes are differentially regulated in response to cytokinin in wild-type roots, but are not regulated in the *php* triple mutant in response to either concentration of cytokinin (Figure 5c,d). For example, 747 genes are significantly upregulated in response to 5- μ M BA in the wild-type rice roots that are not significantly differentially expressed in response to cytokinin in *php1,2,3* mutant roots. However, most of these genes fall into one of two categories. The first are genes that are expressed at very low levels (i.e., relatively few counts detected, though above the minimal to be considered expressed) and therefore may represent false positives/negatives (Table S4). A second class of genes are similar to many of the type-A RRs in that these genes show an elevated level of expression in the *php1,2,3* mutant roots as compared with the wild type in the absence of exogenous cytokinin, but similar levels of expression in the presence of exogenous BA; therefore, these genes are less/not induced in the mutant (Table S4). Few genes are not cytokinin induced in *php1,2,3* that show a substantial level of expression (i.e., >20 normalized counts in wild-type roots in the absence of BA) that are not constitutively upregulated in *php1,2,3* mutant roots (Table S4).

DISCUSSION

Cytokinin plays a key role in regulating many processes that are essential to plant growth and development. Phylogenetic analyses show that many components of the canonical cytokinin signaling machinery are well conserved between Arabidopsis and rice (Pils and Heyl, 2009; Tsai *et al.*, 2012). Our research reveals that this is not true of all components of the canonical cytokinin signaling pathway. Although there is a scarcity of fully sequenced plant genomes for many large phylogenetic groups, particularly gymnosperms and early diverging angiosperms, it seems that PHPs, or something that most resembles what we define as a PHP in angiosperms, did not arise until the evolution of certain gymnosperms, such as *Picea abies*. Similar to dicots, *Picea abies* PHPs have an Asn at the location of the His residue, which is the target of phosphorylation in the AHPs, in contrast to the monocots that have a Gln at this position. In angiosperms, monocot and eudicot

PHPs form independent clades that likely share independent evolutionary origins, with the monocot PHPs being more closely related to AHP4 than any other dicot PHP. The function of AHP4 in Arabidopsis is not well understood and there is evidence that it may act as either a positive or negative regulator of cytokinin in different contexts (Hutchison *et al.*, 2006).

Consistent with the observation that the monocot and dicot PHPs most likely arose independently, we observed that the rice PHPs were unable to complement the Arabidopsis *ahp6* mutant phenotype. This inability to complement was not due to a change in amino acids at the position usually occupied by the conserved His, as swapping this residue between PHP1 of rice and AHP6 of Arabidopsis did not affect the ability of either protein to complement an Arabidopsis *ahp6* mutant.

Not only are these genes not orthologous, but they are under the control of different regulatory inputs. In Arabidopsis, AHP6 is highly induced by auxin (Bishopp *et al.*, 2011) and consequently its expression in roots is restricted to the protoxylem. In contrast, the rice PHPs are not induced by auxin (Tsai *et al.*, 2012). Here, we report that the expression of PHPs in rice roots is much broader than that of AHP6 in Arabidopsis roots with the signal being observed for PHP1 in the procambium and inner cortex, and for PHP2 and PHP3 in the epidermis. Together with the mutant phenotypes uncovered here, these differences in expression patterns demonstrate that the rice PHPs have not only evolved to regulate a set of processes discrete from AHP6 of Arabidopsis, but are regulated themselves by different inputs. It will be interesting for future research to investigate whether the rice PHPs are induced by specific internal signals, such as different phytohormones, or if their expression is under the control of external stimuli, such as changes in environmental inputs, as recently, Arabidopsis AHP4 has been shown to influence growth and development under water deficit (Ha *et al.*, 2020). Rice PHPs are also expressed in shoots and panicles, and regulate shoot growth, inflorescence architecture and seed fill, phenotypes that have not been associated with AHP6 in Arabidopsis, showing a clear difference in the processes that they regulate, although AHP4 has been linked to secondary thickening of the anther endothecium (Jung *et al.*, 2008).

To pursue whether the PHPs function by modulating cytokinin signaling output, we performed RNA-Seq analysis on *php* mutant roots. Despite the fact that we could not discern any root phenotypes, we observed 519 differentially expressed genes between the mutant and wild-type roots. These showed strong overlap with genes that are known to be cytokinin regulated. While it is possible that the PHP proteins have some functions independent of cytokinin signaling, these results make it clear that they function at least in part by modulating the response to

cytokinin. Disruption of the PHPs in roots leads to an upregulation of other negative regulators of cytokinin function, including the type-A *RRs*, multiple *CKX* genes, and a *cisZOG1* paralog. The compensatory upregulation of these negative regulators likely mutes the phenotypic consequences of the *php* triple loss-of-function mutant and suggests potential functional redundancy among these negative regulators. Indeed, when we profiled cytokinin levels in spikelets, we observed a shift in the relative levels of different isoforms, consistent with a feedback on cytokinin homeostasis. This compensatory upregulation may be tissue-specific, as while a *cisZOG1* paralog was induced in roots, we did not observe a significant difference in the quantity of *O*-glucosyl-*cis*-zeatin in spikelets.

It is interesting that the *php1,2,3* triple mutant had little effect on the cytokinin response when plants were treated with high levels of cytokinin. This suggests that a system must exist where different negative regulators function depending on the concentration of cytokinin within a cell. Our results suggest that the PHP proteins reduce cytokinin signaling only at endogenous levels of cytokinin. In the presence of high levels of cytokinin (i.e., exogenous cytokinin), the negative effect of the PHPs is negligible as we observed little or no difference in the response to exogenous cytokinin in molecular and root growth assays. This suggests when the flux of phosphate through the cytokinin-regulated phosphorelay is low, the PHPs can reduce the ultimate transfer to the type-B *RRs*, therefore dampening the cytokinin signaling output. In contrast, in the presence of high cytokinin levels, the phospho flux through the pathway is likely too high to be reduced effectively by the PHPs. Similar RNA-Seq experiments following cytokinin induction have not been published on Arabidopsis *ahp6* mutants, and therefore it is not possible to know whether this concentration-based effect on cytokinin repression is unique to the PHPs or whether AHP6 acts in a similar manner. Nevertheless, together with our phylogenetic analysis, these observations suggest that the PHPs evolved from AHPs at least twice, and in both cases, these molecules have switched from being positive regulators of cytokinin signaling to become inhibitors. Although all the monocot PHPs form one distinct clade, it will be interesting for future studies to confirm whether PHPs from other monocot plants share the same functions, particularly in species where the panicle architecture is somewhat different from rice.

This work also raises the question regarding what components regulate processes such as vascular patterning in monocots. Recent modeling work suggests that the mutually inhibitory interaction between auxin and cytokinin that regulates vascular pattern in Arabidopsis can produce patterns more similar to those observed in rice as the diameter of the root increases (Mellor *et al.*, 2019). However, a central tenet underlying this is the presence of an auxin-inducible inhibitor of cytokinin that would play an AHP6-like

role (Bishopp *et al.*, 2011). As the rice PHPs do not function like AHP6 to inhibit cytokinin at the protoxylem to facilitate xylem formation, and are not induced by auxin (Tsai *et al.*, 2012), a future question will be whether other molecules have evolved such a role. One candidate is the type-A *RR OsRR7*, as this is auxin inducible in both roots and shoots (Tsai *et al.*, 2012) and inhibits cytokinin signaling. It is fascinating that individual components of the gene regulatory networks that control vascular patterning are not well conserved between plants.

EXPERIMENTAL PROCEDURES

Gene accession numbers

For all gene designations, we used the RAP-DB (Rice Annotation Project Database: <https://rapdb.dna.affrc.go.jp/index.html>). The gene accession numbers for the PHPs are *PHP1* (Os01g0743800), *PHP2* (Os05g0186100), and *PHP3* (Os05g0521300).

Phylogenetic analysis

Primary transcript protein sequence databases were downloaded for a subset of species from Phytozome v13 (<https://phytozome-next.jgi.doe.gov/>) (Goodstein *et al.*, 2011). Sequence files for other lineages not available through Phytozome were downloaded to supplement the breadth of lineages searched (full list of species and IDs in Table S2). Gymnosperm sequences were obtained from congenie.org (Nystedt *et al.*, 2013). The *P. obtusifolia* transcriptome was modified (trimmed using a custom perl script, quality-assessed with BUSCO/3.1.0 (Simão *et al.*, 2015; Waterhouse *et al.*, 2017), and translated using TRANSDCODER/2.1.0 (Haas *et al.*, 2013; Batista *et al.*, 2017). *Azolla filiculoides* and *Saccostrea cucullata* were downloaded from <ftp://ftp.fernbase.org/> (Li *et al.*, 2018). *Combrethrum micranthum* was downloaded from NCBI (Chaw *et al.*, 2019). A profile HMM was built using amino acid sequences for the known HPs from *Arabidopsis thaliana* and rice using hmmbuild (HMMER/3.2.1) (Eddy, 1998), and was used to mine the protein sequence databases using HMMSEARCH (HMMER/3.2.1) (Eddy, 1998) with -T 101. This resulted in a master list, which contained both AHPs and PHP sequences. The amino acid sequence for YPD1 (UniProtKB, ID Q07688), a phosphotransfer protein from *Saccharomyces cerevisiae*, was included in this list as a root for downstream phylogenetic analyses. We note that, previously, the default -T was used in HMMSEARCH and additional proteins were recovered, including two from *A. thaliana* (AT4G04402 and AT5G19710) and one from *P. patens* (Pp3c23_13840V3.1.p). We determined through sequence alignment that these proteins are not well conserved enough to be considered AHPs or PHPs and decided to use a more stringent cutoff value in our searches.

Sequences were aligned using MAFFT/7.305 (Katoh *et al.*, 2017), and visualized in JALVIEW 2 (Waterhouse *et al.*, 2009). Coloration of amino acid residues in alignments follows that of CLUSTAL (<http://www.jalview.org/help/html/colourSchemes/clustal.html>). Phylogenetic trees were constructed using RAxML/8.2.11 (Stamatakis, 2006). MAFFT alignments were used as input, and an ML tree was constructed using the following options: `f a -N 100 -m PROTGAM-MAAUTO -p 12345 -x 12345`. Trees were visualized in FIGTREE v1.4.4 (<http://tree.bio.ed.ac.uk/software/figtree/>). To create the abbreviated tree and alignment for Figure 1(a), we chose one to two species each of representative monocots and dicots, one representative gymnosperm and one bryophyte. Sequences were

aligned and the phylogenetic tree was built and visualized as above.

Protein purification

Constructs for expression of SLN1-HK and SLN1-Rec of yeast (Janiak-Spens *et al.*, 1999; Ault *et al.*, 2002b) with GST tags were obtained from Ann West (University of Oklahoma). The CDS of *AHP1*, *PHP1*, *PHP2* and *PHP3* were amplified from rice (cultivar Nipponbare) cDNA (for primers, see Table S8) using Phusion DNA polymerase (New England Biolabs, Ipswich, MA, USA). *AHP1* was cloned into pGEX-6p1 (Mähönen *et al.*, 2006) (obtained from Tatsuo Kakimoto, Osaka University) and *PHP1*, *PHP2* and *PHP3* were cloned into pFAST-BAC1-GST. Site directed mutagenesis was performed to restore the conserved phosphoaccepting His residue of *PHP1*, *PHP2* and *PHP3*, using the Quickchange II XL kit (Agilent Technologies, Santa Clara, CA, USA) (See Table S8 for primers).

SLN1-HK, SLN1-Rec and rice *AHP1* were expressed and purified from the *Escherichia coli* strain Origami 2(DE3)pLysS (Novagen, Darmstadt, Germany). Cells were grown for 2 h after induction and harvested by centrifugation at 4000 *g* for 15 min. Cell pellets were resuspended in 40 ml of GST buffer (50 mM Tris-HCl pH 8, 150 mM NaCl, 1 mM EDTA, 10% v/v glycerol, β -mercaptoethanol, 1 mM 4-(2-aminoethyl)benzenesulfonyl fluoride hydrochloride (AEBSF), 10 μ g ml⁻¹ leupeptin) and then lysed using a high pressure cell disruptor at 35 kPa. The lysate was centrifuged at 4000 *g* for 15 min at 4°C and the supernatant decanted and centrifuged at 45 000 *g* for 1 h at 4°C. The GST tagged proteins were purified using glutathione Sepharose 4B resin as described by the manufacturer (Cytiva, Marlborough, MA, USA). GST tagged proteins were eluted with 500 μ l of 40 mM glutathione in GST buffer; GST tagged SLN1-HK and SLN1-Rec protein was left bound to glutathione Sepharose 4B beads and used in assays as such. Buffers in purified samples were exchanged for phosphotransfer buffer (50 mM Tris-HCl pH 8, 50 mM KCl, 10% v/v glycerol, 2 mM β -mercaptoethanol, 0.1 mM AEBSF) by dialysis.

PHP1, *PHP2* and *PHP3* from rice were expressed and purified using Sf9 cells with the Bac-to-Bac expression system as described by the manufacturer (Thermo Fisher, Waltham, MA, USA). Briefly, pFAST-BAC1-GST plasmids containing CDS of genes to be expressed were used to transform *E. coli* strain DH10Bac. These cells are used to synthesize recombinant bacmid, which was extracted and used to infect Sf9 cells. Sf9 cells were maintained in mid-log phase and grown at 28°C in Insect X-Press protein-free media with L-glutamine (Lonza, Basel, Switzerland) and supplemented with penicillin (100 U ml⁻¹) and streptomycin (100 μ g ml⁻¹). For infection with bacmid, insect cells were grown as a monolayer adhered to the bottom of six-well plates; for all other infections, cells were grown in media shaking at 150 rpm with 10% fetal calf serum. Infections were carried out according by the manufacturer (Thermo Fisher). Baculovirus-infected insect cell stocks were made as previously described (Wasilko *et al.*, 2009). For protein purification, 200 ml cultures (seeded at 0.5 \times 10⁶ cell ml⁻¹ and grown for 24 h before infection) were infected with 100 μ l baculovirus-infected insect cell stock. After expression of protein in insect cells, cultures were pelleted by centrifuging at 4000 *g* for 15 min and resuspended in 20 ml GST buffer. Cells were lysed using a probe sonicator and protein purified as described above.

Phosphotransfer assays

Phosphotransfer assays were carried out as described (Fassler and West, 2010). For phosphorylation of bead-bound SLN1-HK,

3 μ M of bead bound protein was combined with 7 μ M [γ -³²P]-ATP (30 Ci/mmol) in phosphotransfer buffer (50 mM Tris-HCl pH 8, 100 mM KCl, 10 mM MgCl₂, 2 mM DTT, 20% glycerol) and incubated at room temperature for 1 h. Resin-bound phosphorylated protein was pelleted by centrifuging at 100 *g* for 1 min and washed three times with wash buffer (50 mM Tris-HCl pH 8, 50 mM KCl, 10 mM MgCl₂, 1 mM DTT). The pellet was resuspended in 100 μ l of wash buffer and used in phosphotransfer experiments immediately.

To follow transfer of the phosphate group from SLN1-HK to HPs, ³²P-SLN1-HK-Rec was incubated with HPs in equimolar amounts in a total reaction volume of 15 μ l in reaction buffer (50 mM Tris-HCl pH 8, 30 mM KCl, 10 mM MgCl₂, 1 mM DTT) for 10 min at room temperature. Reactions were stopped by adding 5 μ l of 4 \times stop buffer (250 mM Tris-HCl pH 6.8, 8% sodium dodecyl sulfate, 60 mM EDTA, 40% glycerol, 0.008% bromophenol blue), samples run by polyacrylamide gel electrophoresis, the wet gel sealed and exposed to a BAS-IP-MS storage phosphor sheet (GE Healthcare, Chicago, IL, USA) and imaged using the molecular imager FX (Bio-Rad, Hercules, CA, USA).

Complementation of Arabidopsis *ahp6* mutants

Vectors for *trans*-complementation experiments were constructed using MultiSite Gateway (Invitrogen, Waltham, MA, USA). CDS from *PHP1*, *PHP2* and *PHP3* from rice and *AHP6* from Arabidopsis were amplified from cDNA (for primers, see Table S8) with Phusion DNA polymerase (New England Biolabs), and cloned into pDONR_221. Resulting entry clones were confirmed by sequencing and recombined with the entry clones pDONR_P4P1R_*AHP6* and p2RP3_nosT2 into the destination vector pHm34GW through an LR reaction. Recombined vector junctions were confirmed by sequencing. *AHP6*(NQ) substitution was created by site-directed mutagenesis using the Quickchange II XL kit (Agilent Technologies) (for primers, see Table S8). *PHP1*(QN) substitution was created using Gibson assembly cloning with Gibson Assembly master mix (New England Biolabs) according to the manufacturer's instructions. Complementation vectors were transformed into Arabidopsis *ahp6-2* mutants and at least three independent transgenic lines in the T3 generation were used for phenotyping analysis. For phenotyping, 5-day-old seedlings were mounted in chloral hydrate and primary roots scored for xylem defects. At least 20 plants were scored for each independent line. For better imaging of *ahp6* mutant xylem defects, 5-day-old seedlings of Col-0, *ahp6-2* mutants were harvested and incubated in acidified methanol (20% methanol and 4 N HCl) at 55°C for 15 min, then basic solution (7% NaOH in 60% ethanol) at room temperature for 15 min. Samples were then rehydrated sequentially in 40%, 20% and 10% ethanol for 30 min each, stained in 0.01% basic Fuchsin for 5 min, and then de-stained in 70% ethanol for 10 min. Seedlings were rehydrated by incubating in 40%, 20% and 10% ethanol for 10 min, followed by 5% ethanol 25% glycerol overnight. Samples were then mounted in 5% glycerol and imaged using a Leica SP5 confocal microscope.

Transcriptional reporters

Promoter regions 3 kb immediately upstream of the start codon for *PHP1*, *PHP2* and *PHP3* were amplified from rice (cultivar Kitaake) gDNA using Phusion DNA polymerase (New England Biolabs) and cloned into pCambia 1305.1 (Curtis and Grossniklaus, 2003). For GUS staining, tissue was harvested and fixed in cold acetone for 1 h on ice. Acetone was washed out of tissue with multiple washes of sodium phosphate buffer monobasic (100 mM, pH 7). Tissue was then placed in GUS stain solution (1 mM EDTA pH 8, 5 mM potassium ferricyanide, 5 mM potassium ferrocyanide,

0.1% Triton-X-100, 1 mg ml⁻¹ X-gluc) and incubated at 37°C in the dark until staining appeared. After an appropriate amount of staining was seen, GUS stain solution was removed and replaced with 70% (v/v) ethanol for 1 day. Tissue was then mounted in chloral hydrate and imaged.

For embedding and sectioning in plastic resin after GUS staining, dissected roots were fixed in 5 ml fixation solution (1 ml 25% glutaraldehyde, 2.7 ml 37% formaldehyde, 2.5 ml 0.5 M NaPi pH 7.2, 18.8 ml double-distilled H₂O) overnight at 4°C. Tissue was then taken through an ethanol dilution series of 10%, 30%, 50%, 70%, 96% and 100%, and again 100% ethanol with incubations of 30 min at each dilution. Tissue was then incubated in 1:1 100% ethanol/Solution A (Leica HistoResin embedding kit) and incubated at room temperature overnight. Tissue was then incubated in Solution A for 4 h and transferred to molds filled with 15:1 Solution A/Hardener (Leica HistoResin embedding kit), which were left to set fully. Embedded tissue was sectioned (4 µm sections) using a Leica Ultracut EM UC6 microtome. Sections were stained with 0.05% toluidine blue in 0.1 M sodium phosphate buffer and imaged using a Leica DM5000 B microscope.

Creation of CRISPR mutant lines

CRISPR/Cas9 guide RNAs were designed to target *PHP1*, *2* and *3* using CRISPR-PLANT (<https://www.genome.arizona.edu/crispr/index.html>) (Xie *et al.*, 2014). In-Fusion cloning primers were designed so that each CRISPR target sequence would be created between the rice pU3 promoter and *Setaria* U6 guide RNA sequence on completion of the In-Fusion reaction (Takara, Kusatsu, Shiga, Japan). The CRISPR/Cas9 guide RNAs were ligated into pARS3_MUbcas9_MC (Worthen *et al.*, 2019), creating a multiplexed CRISPR vector, which was transformed into *Agrobacterium* strain EHA101. Rice callus (cultivar Kitaake) was transformed with *Agrobacterium* strain EHA101 containing the *PHP* CRISPR vector at the transformation facility at Iowa State University (<https://www.biotech.iastate.edu/biotechnology-service-facilities/plant-transformation-facility/>). Transformants were selected using hygromycin, and 26 resistant individuals, rooted on regeneration medium II, were transplanted to soil. These plantlets were grown up in soil (10 h light/14 h dark; 27.5°C/23.5°C) and screened for CRISPR activity, as described below. Seed was taken from individuals with active editing and screened for *php* mutations by amplifying target genes using polymerase chain reaction followed by acrylamide gel electrophoresis (for primer sequences, see Table S8) and mutations confirmed by Sanger sequencing. The CRISPR/Cas9 transgene was segregated out of the mutants used in further analyses.

Morphological assays

Morphological assays of rice were performed in three replicates. Wild-type and *php1,2,3* triple mutant seeds were dehusked and sterilized with 50% bleach (Clorox) solution by incubating with shaking at room temperature for 30 min. The seeds were then rinsed six times with sterile water and moved to a petri dish with moistened sterile filter paper and germinated overnight at 37°C. The seeds were then transferred directly to soil in 4 × 4 × 10 inch pots and grown in a greenhouse (13 h light/11 h dark, 28°C/25°C, with supplemental lighting (450 W M⁻²) when needed). At 10 weeks, all stems with emerged panicles were marked and the plants were left to continue developing. At 4 months, the grain on the selected panicles was fully mature and the marked stems were used to collect phenotypic data. Internode lengths were measured, starting at the root/shoot barrier measuring each internode, until the shoot/panicle barrier was reached. Panicles were measured

starting from the shoot/panicle barrier to the uppermost seed on the panicle. Total stem height was determined by adding each internode length and the panicle length. Primary, secondary and tertiary branches were quantified for each panicle. Lastly, total spikelet count per panicle was determined and filled spikelets were counted.

Morphological data analyses, graphing and statistical analyses were performed using R 3.6.1 and RStudio Version 1.2.5001. The data from the three replicates were visualized and the appropriate statistical test was applied using the ggstatsplot package in R to compare Kitaake and *php1,2,3* across the different morphological features. $P < 0.01$ was considered significant. Measurements from the three replicates were not averaged.

For root phenotyping of the rice *php* triple mutant, seedlings were grown sterile on agar plates and imaged after 14 days. Root architectural measures were calculated using ROOTNAV software from 18 plants per genotype (Pound *et al.*, 2013). For analysis of root anatomy, at least nine plants per genotype were sectioned 5 cm above the root tip using a vibratome. Primary and crown roots were harvested and embedded in 3% agarose. Samples were then mounted on to the vibratome block and 100 µm sections cut. Sections were stained with calcofluor white for 30 sec, washed in water and imaged using a Nikon confocal microscope with three sequential scans with different laser and detector combinations to create three overlaid images (1: laser 488 and 543, detector 605/75; 2: laser 408, detector 450/35; 3: laser 408, detector 515/30). Anatomical measurements were taken using PHIV ROOTCELL software (Lartaud *et al.*, 2015).

Cytokinin response assays

Seeds were sterilized with bleach for the morphological assay. After overnight germination at 37°C, seeds with an emerged coleoptile were transferred to 1× Kimura B Nutrient solution, pH 5.5 (pH adjusted using 1 M KOH) (Ma *et al.*, 2001) solidified with 0.6% Phytigel (Sigma, St. Louis, MO, USA) in Dart Solo RTP16DBARE cups capped with Dart Solo DLW626 lids in which the holes were sealed with a sterile foam stopper (250 ml media per cup). BA at various concentrations or a vehicle control (NaOH) was added to each sample. Six seeds were transplanted into each cup and were grown for 7 days (10 h light/14 h dark; 27.5°C/23.5°C). On day 7, the plants were photographed and primary root length, crown root number and shoot length measured using ImageJ software (Schneider *et al.*, 2012).

Quantification of cytokinins

Spikelets were collected at flowering and flash frozen in liquid nitrogen. For total cytokinin content analysis, an average 30 mg fresh weight material was used per sample (individual plant, $n = 10$). Samples were extracted in modified Bielecki buffer (methanol/water/formic acid, 15/4/1, v/v/v) with a mixture of stable isotope-labeled CK internal standards added to each sample for precise quantification (Hoyerová *et al.*, 2006). The purification of isoprenoid CKs was carried out according to Dobrev and Kaminek (2002) using the MCX column (30 mg of C18/SCX combined sorbent with cation-exchange properties). Analytes were eluted by two-step elution using a 0.35 M NH₄OH aqueous solution and 0.35 M NH₄OH in 60% (v/v) MeOH solution. Samples were then evaporated to dryness under vacuum at 37°C. Prior to analysis, the samples were dissolved in 40 µl, 10% MeOH. Mass spectrometry (MS) analysis and quantification were performed using an liquid chromatography (LC)-MS/MS system consisting of a 1290 Infinity Binary LC System coupled to a 6490 Triple Quad LC/MS System with Jet Stream and Dual Ion Funnel technologies (Agilent

Technologies). Ultrahigh-performance liquid chromatography-electrospray ionization-MS/MS method parameters were adapted from Svacinová *et al.* (2012).

RNA-Seq analysis

Rice seeds were surface sterilized in 50% bleach (Clorox) for 30 min and grown in sterilized hydroponics chambers for 1 week in liquid Kimura media in constant light at 27°C. One day before treatment, the media in the hydroponics boxes was replaced with fresh media and sterile air pumped through the hydroponic chamber continually through to the end of the experiment. Either a vehicle control (NaOH) or a BA treatment (100 nM or 5 µM BA, in 5 M NaOH solution) was added to the media for 2 h. A set of approximately eight developmentally matched seedlings were chosen from each genotype at each treatment condition. The roots were separated from the shoots using a scalpel blade by cutting above and below germinated rice. The root tissue was sliced several places along its length and then mixed so that each sample would contain a mix of root fragments from each plant and from each region of the root. The shoots were cut and mixed the same way. Each set of root and shoot tissue was divided into three technical replicates and flash frozen in liquid nitrogen. Three biological replicates were gathered in total.

RNA was prepared using an RNeasy Mini Kit (Qiagen, Hilden, Germany) and libraries prepared using Kapa TruSeq adapters as described (Lundberg *et al.*, 2013). Samples were evenly pooled on one flow cell of a NovaSeq SP and paired-end 50-bp sequences were generated. Alignment was performed using a “star” (Dobin *et al.*, 2012) genome built on the IRGSP 1.0 genome release and an IRGSP 1.0 representative transcript file (created on August 29, 2019). An overhang value of 49 was used and based on recommendations from the program, the SA index N bases parameter was set to 13. Quantification was performed using “salmon” (Patro *et al.*, 2017) and the same transcriptome file used for the “star” index. The gcBias and seqBias flags were both activated. The “star” version was 2.7.2b and the “salmon” version was v0.14.0. Differential expression analysis was performed in “R” v3.6.1 using “DESeq2” (Love *et al.*, 2014) v1.24.0. *P*-value adjustment was performed using the independent hypothesis weighting package in R (Ignatiadis *et al.*, 2016). An FC cutoff of 1.5 was imposed on the data by comparing the similarity between sets of DE genes in the 100 nM and 5 µM BA Kitaake samples using a Jaccard index, similar to the between-replicates strategy proposed by Rau *et al.* for choosing optimal gene filters (Rau *et al.*, 2013).

For Gene Ontology term enrichment analysis, g:Profiler (version e101_eg48_p14_baf17f0) was used with the default options (Raudvere *et al.*, 2019).

CODE AVAILABILITY

The code used in this study can be accessed on Github (<https://github.com/KieberLab/Cytokinin-RICE>).

ACKNOWLEDGEMENTS

This work was supported by grants from the NSF to JJK and GES (IOS-1238051 and MCB-1856248) and the USDA to JJK (2018-67013-27423). JVH was supported by as part of the BBSRC Doctoral Training Program and through a PhDPlus award as part of the UoN Beacon for Future Food. RB is supported by BBSRC Discovery and Future Food Beacon Nottingham Research Fellowships. AB is supported by a Royal Society URF, and a Marie Curie CIG. We would like to thank Augustus Elmore for technical assistance with the rice analysis, as well as Jamie Winshell for overall

technical support. KL and JS were supported by grants from the Swedish Research Councils VR, Kempefistelserna, and the Knut and Alice Wallenberg Foundation. We thank the Swedish Metabolomics Center (SMC, Umeå, Sweden) for access to instrumentation.

AUTHOR CONTRIBUTIONS

EJ, J V-H, CB, KL, GES, AB and JJK conceptualized and designed research. EJ, JV-H, CB, CH, SLB, IK, WL, AM, DX, KB, JS, KS and RB conducted experiments. CH, IK, WL, RB and JJK analyzed RNA-Seq data. JV-H, EJ, AB and JJK wrote the manuscript with input from the other authors.

CONFLICT OF INTEREST

The authors declare that they have no competing interests.

DATA AVAILABILITY STATEMENT

The raw and processed RNA-Seq data described in this study have been deposited to the NCBI Short Read Archive (SRA) database under PRJNA589193 and Gene Expression Omnibus under Series GSE141408, respectively.

SUPPORTING INFORMATION

Additional Supporting Information may be found in the online version of this article.

Figure S1. Phylogenetic relationship among His phosphotransfer proteins across Viridiplantae.

Figure S2. Multiple sequence alignment for all putative PHPs proteins from Figure S1.

Figure S3. Spatial expression pattern of *PHP1-PHP3*.

Figure S4. Analysis of root cross-sections.

Figure S5. Analysis of root architecture in wild-type and *php* mutants

Figure S6. Cytokinin response assay of wild-type and *php* seedlings

Figure S7. Expression of type-A *RRs* and *CKX* genes in wild-type and *php1,2,3* mutant roots.

Table S1. Gene annotations for genes used in Figure 1(a,b).

Table S2. Gene annotations for genes used in Figure S1.

Table S3. Quantification of various cytokinin species in wild-type and *php1,2,3* mutant spikelets.

Table S4. DEGs in response to exogenous cytokinin in wild-type and *php1,2,3* roots.

Table S5. Expression of genes encoding proteins involved in cytokinin signaling or metabolism in wild-type and *php1,2,3* mutant roots.

Table S6. DEGs between wild-type and *php1,2,3* roots.

Table S7. Gene Ontology enrichment analysis of genes differentially expressed in *php1,2,3* mutant as compared with wild-type roots.

Table S8. Primers used in the study.

REFERENCES

Andersen, T.G., Naseer, S., Ursache, R., Wybouw, B., Smet, W., De Rybel, B., Vermeer, J.E.M. and Geldner, N. (2018) Diffusible repression of cytokinin signalling produces endodermal symmetry and passage cells. *Nature*, **555**, 529–533.

- Argyros, R.D., Mathews, D.E., Chiang, Y.H., Palmer, C.M., Thibault, D.M., Etheridge, N., Argyros, D.A., Mason, M.G., Kieber, J.J. and Schaller, G.E. (2008) Type B response regulators of Arabidopsis play key roles in cytokinin signaling and plant development. *Plant Cell*, **20**, 2102–2116.
- Ashikari, M., Sakakibara, H., Lin, S., Yamamoto, T., Takashi, T., Nishimura, A., Angeles, E.R., Qian, Q., Kitano, H. and Matsuoka, M. (2005) Cytokinin oxidase regulates rice grain production. *Science*, **309**, 741–745.
- Ault, A.D., Fassler, J.S. and Deschenes, R.J. (2002a) Altered phosphotransfer in an activated mutant of the *Saccharomyces cerevisiae* two-component osmosensor Sln1p. *Eukaryot. Cell*, **1**, 174–180.
- Bartrina, I., Otto, E., Strnad, M., Werner, T. and Schmülling, T. (2011) Cytokinin regulates the activity of reproductive meristems, flower organ size, ovule formation, and thus seed yield in *Arabidopsis thaliana*. *Plant Cell*, **23**, 69–80.
- Batista, A.N.L., Santos-Pinto, J.R.A.D., Batista, J.M., Souza-Moreira, T.M., Santoni, M.M., Zanelli, C.F., Kato, M.J., López, S.N., Palma, M.S. and Furlan, M. (2017) The combined use of proteomics and transcriptomics reveals a complex secondary metabolite network in *Peperomia obtusifolia*. *J. Nat. Prod.* **80**, 1275–1286.
- Besnard, F., Refahi, Y., Morin, V. et al. (2014) Cytokinin signalling inhibitory fields provide robustness to phyllotaxis. *Nature*, **505**, 417–421.
- Bishopp, A., Help, H., El-Showk, S., Weijers, D., Scheres, B., Friml, J., Benková, E., Mähönen, A. and Helariutta, Y. (2011) A mutually inhibitory interaction between auxin and cytokinin specifies vascular pattern in roots. *Curr. Biol.* **21**, 927–932.
- Brandstatter, I. and Kieber, J.J. (1998) Two genes with similarity to bacterial response regulators are rapidly and specifically induced by cytokinin in Arabidopsis. *Plant Cell*, **10**, 1009–1020.
- Burr, C.A., Sun, J., Yamburenko, M.V. et al. (2020) The HK5 and HK6 cytokinin receptors mediate diverse developmental pathways in rice. *Development*, **147**(20), dev191734.
- Chaw, S.-M., Liu, Y.-C., Wu, Y.-W. et al. (2019) Stout camphor tree genome fills gaps in understanding of flowering plant genome evolution. *Nat. Plants*, **5**, 63–73.
- Curtis, M.D. and Grossniklaus, U. (2003) A gateway cloning vector set for high-throughput functional analysis of genes in planta. *Plant Physiol.* **133**, 462–469.
- D'Agostino, I., Deruère, J. and Kieber, J.J. (2000) Characterization of the response of the Arabidopsis *ARR* gene family to cytokinin. *Plant Physiol.* **124**, 1706–1717.
- Ding, W., Tong, H., Zheng, W., Ye, J., Pan, Z., Zhang, B. and Zhu, S. (2017) Isolation, characterization and transcriptome analysis of a cytokinin receptor mutant *Oscck1* in rice. *Front. Plant Sci.* **8**, 88.
- Dobin, A., Davis, C.A., Schlesinger, F., Drenkow, J., Zaleski, C., Jha, S., Batut, P., Chaisson, M. and Gingeras, T.R. (2012) STAR: ultrafast universal RNA-seq aligner. *Bioinformatics*, **29**, 15–21.
- Dobrev, P.I. and Kaminek, M. (2002) Fast and efficient separation of cytokinins from auxin and abscisic acid and their purification using mixed-mode solid-phase extraction. *J. Chromatogr. A*, **950**, 21–29.
- Du, L., Jiao, F., Chu, J., Chen, M. and Wu, P. (2007) The two-component signal system in rice (*Oryza sativa* L.): a genome-wide study of cytokinin signal perception and transduction. *Genomics*, **89**, 697–707.
- Eddy, S.R. (1998) Profile hidden Markov models. *Bioinformatics*, **14**, 755–763.
- Fassler, J.S. and West, A.H. (2010) Genetic and biochemical analysis of the SLN1 pathway in *Saccharomyces cerevisiae*. *Methods Enzymol.* **471**, 291–317.
- Goodstein, D.M., Shu, S., Howson, R. et al. (2011) Phytozome: a comparative platform for green plant genomics. *Nucl. Acids Res.* **40**, D1178–D1186.
- Gu, B., Zhou, T., Luo, J. et al. (2015) An-2 encodes a cytokinin synthesis enzyme that regulates awn length and grain production in rice. *Mol. Plant*, **8**, 1635–1650.
- Ha, C.V., Nguyen, K.H., Mostofa, M.G. et al. (2020) The histidine phosphotransfer AHP4 plays a negative role in Arabidopsis plant response to drought. *bioRxiv*, <https://doi.org/10.1101/2020.07.30.229971>.
- Haas, B.J., Papanicolaou, A., Yassour, M. et al. (2013) De novo transcript sequence reconstruction from RNA-seq using the Trinity platform for reference generation and analysis. *Nat. Protoc.* **8**, 1494.
- Higuchi, M., Pischke, M.S., Mahonen, A.P. et al. (2004) In planta functions of the Arabidopsis cytokinin receptor family. *Proc. Natl Acad. Sci. USA*, **101**, 8821–8826.
- Hirose, N., Makita, N., Kojima, M., Kamada-Nobusada, T. and Sakakibara, H. (2007) Overexpression of a type-A response regulator alters rice morphology and cytokinin metabolism. *Plant Cell Physiol.* **48**, 523–539.
- Hoyerová, K., Gaudinová, A., Malbeck, J., Dobrev, P.I., Kocáček, T., Solcová, B., Trávníčková, A. and Kaminek, M. (2006) Efficiency of different methods of extraction and purification of cytokinins. *Phytochemistry*, **67**, 1151–1159.
- Hutchison, C.E. and Kieber, J.J. (2007) Signaling via histidine-containing phosphotransfer proteins in Arabidopsis. *Plant Signal Behav.* **2**, 287–289.
- Hutchison, C.E., Li, J., Argueso, C. et al. (2006) The Arabidopsis histidine phosphotransfer proteins are redundant positive regulators of cytokinin signaling. *Plant Cell*, **18**, 3073–3087.
- Hwang, I., Sheen, J. and Müller, B. (2012) Cytokinin signaling networks. *Annu. Rev. Plant Biol.* **63**, 353–380.
- Ignatiadis, N., Klaus, B., Zaugg, J.B. and Huber, W. (2016) Data-driven hypothesis weighting increases detection power in genome-scale multiple testing. *Nat. Methods*, **13**, 577–580.
- Jain, M., Tyagi, A.K. and Khurana, J.P. (2006) Molecular characterization and differential expression of cytokinin-responsive type-A response regulators in rice (*Oryza sativa*). *BMC Plant Biol.* **6**, 1.
- Jameson, P.E. and Song, J. (2016) Cytokinin: a key driver of seed yield. *J. Exp. Bot.* **67**, 593–606.
- Janiak-Spens, F., Cook, P.F. and West, A.H. (2005) Kinetic analysis of YPD1-dependent phosphotransfer reactions in the yeast osmoregulatory phosphorelay system. *Biochemistry*, **44**, 377–386.
- Janiak-Spens, F., Sparling, J.M., Gurfinkel, M. and West, A.H. (1999) Differential stabilities of phosphorylated response regulator domains reflect functional roles of the yeast osmoregulatory SLN1 and SSK1 proteins. *J. Bacteriol.* **181**, 411–417.
- Jung, K.W., Oh, S.I., Kim, Y.Y., Yoo, K.S., Cui, M.H. and Shin, J.S. (2008) Arabidopsis histidine-containing phosphotransfer factor 4 (AHP4) negatively regulates secondary wall thickening of the anther endothecium during flowering. *Mol. Cells*, **25**, 294–300.
- Katoh, K., Rozewicki, J. and Yamada, K.D. (2017) MAFFT online service: multiple sequence alignment, interactive sequence choice and visualization. *Brief. Bioinform.* **20**, 1160–1166.
- Kieber, J.J. and Schaller, G.E. (2014) Cytokinins. *Arabidopsis Book*, **12**, e0168.
- Kieber, J.J. and Schaller, G.E. (2018a) Cytokinin metabolism and signaling. *Development*, **145**(4):dev149344. in press.
- Kieber, J.J. and Schaller, G.E. (2018b) Cytokinin signaling in plant development. *Development*, **145**, dev149344.
- Kudo, T., Makita, N., Kojima, M., Tokunaga, H. and Sakakibara, H. (2012) Cytokinin activity of cis-zeatin and phenotypic alterations induced by overexpression of putative cis-Zeatin-O-glucosyltransferase in rice. *Plant Physiol.* **160**, 319–331.
- Kurakawa, T., Ueda, N., Maekawa, M., Kobayashi, K., Kojima, M., Nagato, Y., Sakakibara, H. and Kyojuka, J. (2007) Direct control of shoot meristem activity by a cytokinin-activating enzyme. *Nature*, **445**, 652–655.
- Lartaud, M., Perin, C., Courtois, B. et al. (2015) PHIV-RootCell: a supervised image analysis tool for rice root anatomical parameter quantification. *Front. Plant Sci.* **5**, 790.
- Li, F.-W., Brouwer, P., Carretero-Paulet, L. et al. (2018) Fern genomes elucidate land plant evolution and cyanobacterial symbioses. *Nat. Plants*, **4**, 460–472.
- Lomin, S.N., Yonekura-Sakakibara, K., Romanov, G.A. and Sakakibara, H. (2011) Ligand-binding properties and subcellular localization of maize cytokinin receptors. *J. Exp. Bot.* **62**, 5149–5159.
- Love, M.I., Huber, W. and Anders, S. (2014) Moderated estimation of fold change and dispersion for RNA-seq data with DESeq2. *Genome Biol.* **15**, 50.
- Lundberg, D.S., Yourstone, S., Mieczkowski, P., Jones, C.D. and Dangl, J.L. (2013) Practical innovations for high-throughput amplicon sequencing. *Nat. Methods*, **10**, 999–1002.
- Ma, J.F., Goto, S., Tamai, K. and Ichii, M. (2001) Role of root hairs and lateral roots in silicon uptake by rice. *Plant Physiol.* **127**, 1773–1780.
- Mähönen, A.P., Bishopp, A., Higuchi, M., Nieminen, K.M., Kinoshita, K., Tormakangas, K., Ikeda, Y., Oka, A., Kakimoto, T. and Helariutta, Y. (2006) Cytokinin signaling and its inhibitor AHP6 regulate cell fate during vascular development. *Science*, **311**, 94–98.

- Mellor, N., Vaughan-Hirsch, J., Kümpers, B.M.C., Help-Rinta-Rahko, H., Miyashima, S., Mähönen, A.P., Campilho, A., King, J.R. and Bishopp, A. (2019) A core mechanism for specifying root vascular patterning can replicate the anatomical variation seen in diverse plant species. *Development*, **146**, dev172411.
- Mok, D.W. and Mok, M.C. (2001) Cytokinin metabolism and action. *Annu. Rev. Plant Physiol. Plant Mol. Biol.* **89**, 89–118.
- Moreira, S., Bishopp, A., Carvalho, H. and Campilho, A. (2013) AHP6 inhibits cytokinin signaling to regulate the orientation of pericycle cell division during lateral root initiation. *PLoS One*, **8**, e56370.
- Müller, C.J., Larsson, E., Spíchal, L. and Sundberg, E. (2017) Cytokinin-auxin crosstalk in the gynoecial primordium ensures correct domain patterning. *Plant Physiol.* **175**, 1144–1157.
- Nishimura, C., Ohashi, Y., Sato, S., Kato, T., Tabata, S. and Ueguchi, C. (2004) Histidine kinase homologs that act as cytokinin receptors possess overlapping functions in the regulation of shoot and root growth in Arabidopsis. *Plant Cell*, **16**, 1365–1377.
- Nystedt, B., Street, N.R., Wetterbom, A. *et al.* (2013) The Norway spruce genome sequence and conifer genome evolution. *Nature*, **497**, 579.
- Pareek, A., Singh, A., Kumar, M., Kushwaha, H.R., Lynn, A.M. and Singla-Pareek, S.L. (2006) Whole-genome analysis of *Oryza sativa* reveals similar architecture of two-component signaling machinery with Arabidopsis. *Plant Physiol.* **142**, 380–397.
- Patro, R., Duggal, G., Love, M.I., Irizarry, R.A. and Kingsford, C. (2017) Salmon provides fast and bias-aware quantification of transcript expression. *Nat. Methods*, **14**, 417–419.
- Pils, B. and Heyl, A. (2009) Unraveling the evolution of cytokinin signaling. *Plant Physiol.* **151**, 782–791.
- Posas, F., Wurgler-Murphy, S.M., Maeda, T., Witten, E.A., Thai, T.C. and Saito, H. (1996) Yeast HOG1 MAP Kinase cascade is regulated by a multi-step phosphorelay mechanism in the SLN1-YPD1-SSK1 “two-component” osmosensor. *Cell*, **86**, 865–875.
- Pound, M.P., French, A.P., Atkinson, J.A., Wells, D.M., Bennett, M.J. and Pridmore, T. (2013) RootNav: navigating images of complex root architectures. *Plant Physiol.* **162**, 1802–1814.
- Raines, T., Blakley, I.C., Tsai, Y.-C., Worthen, J.M., Franco-Zorrilla, J.M., Solano, R., Schaller, G.E., Loraine, A.E. and Kieber, J.J. (2016) Characterization of the cytokinin-responsive transcriptome in rice. *BMC Plant Biol.* **16**, 260.
- Rau, A., Gallopín, M., Celeux, G. and Jaffrézic, F. (2013) Data-based filtering for replicated high-throughput transcriptome sequencing experiments. *Bioinformatics*, **29**, 2146–2152.
- Raudvere, U., Kolberg, L., Kuzmin, I., Arak, T., Adler, P., Peterson, H. and Vilo, J. (2019) g:Profiler: a web server for functional enrichment analysis and conversions of gene lists (2019 update). *Nucl. Acids Res.* **47**(W1), : W191–W198.
- Romanov, G.A., Lomin, S.N. and Schmülling, T. (2006) Biochemical characteristics and ligand-binding properties of Arabidopsis cytokinin receptor AHK3 compared to CRE1/AHK4 as revealed by a direct binding assay. *J. Exp. Bot.* **57**, 4051–4058.
- Sato, Y., Antonio, B.A., Namiki, N., Takehisa, H., Minami, H., Kamatsuki, K., Sugimoto, K., Shimizu, Y., Hirochika, H. and Nagamura, Y. (2011) RiceXPro: a platform for monitoring gene expression in japonica rice grown under natural field conditions. *Nucleic Acids Res.* **39**, D1141–D1148.
- Schaller, G.E., Bishopp, A. and Kieber, J.J. (2015) The yin-yang of hormones: cytokinin and auxin interactions in plant development. *Plant Cell*, **27**, 44–63.
- Schaller, G.E., Doi, K., Hwang, I. *et al.* (2007) Nomenclature for two-component signaling elements of rice. *Plant Physiol.* **143**, 555–557.
- Schneider, C.A., Rasband, W.S. and Eliceiri, K.W. (2012) NIH Image to ImageJ: 25 years of image analysis. *Nat. Methods*, **9**, 671–675.
- Simão, F.A., Waterhouse, R.M., Ioannidis, P., Kriventseva, E.V. and Zdobnov, E.M. (2015) BUSCO: assessing genome assembly and annotation completeness with single-copy orthologs. *Bioinformatics*, **31**, 3210–3212.
- Stamatakis, A. (2006) RAxML-VI-HPC: maximum likelihood-based phylogenetic analyses with thousands of taxa and mixed models. *Bioinformatics*, **22**, 2688–2690.
- Stolz, A., Riefler, M., Lomin, S.N., Achazi, K., Romanov, G.A. and Schmülling, T. (2011) The specificity of cytokinin signalling in Arabidopsis thaliana is mediated by differing ligand affinities and expression profiles of the receptors. *Plant J.* **67**, 157–168.
- Suzuki, T., Imamura, A., Ueguchi, C. and Mizuno, T. (1998) Histidine-containing phosphotransfer (HPT) signal transducers implicated in His-to-Asp phosphorelay in Arabidopsis. *Plant Cell Physiol.* **39**, 1258–1268.
- Suzuki, T., Zakurai, K., Imamura, A., Nakamura, A., Ueguchi, C. and Mizuno, T. (2000) Compilation and characterization of histidine-containing phosphotransmitters implicated in His-to-Asp phosphorelay in plants: AHP signal transducers of *Arabidopsis thaliana*. *Biosci. Biotechnol. Biochem.* **64**, 2482–2485.
- Svačinová, J., Novák, O., Pláčková, L., Lenobel, R., Holík, J., Strnad, M. and Doležal, K. (2012) A new approach for cytokinin isolation from Arabidopsis tissues using miniaturized purification: pipette tip solid-phase extraction. *Plant Methods*, **8**, 17.
- Tan, S., Debellé, F., Gamas, P., Frugier, F. and Brault, M. (2019) Diversification of cytokinin phosphotransfer signaling genes in *Medicago truncatula* and other legume genomes. *BMC Genom.*, **20**, 373.
- Tanaka, Y., Suzuki, T., Yamashino, T. and Mizuno, T. (2004) Comparative studies of the AHP histidine-containing phosphotransmitters implicated in His-to-Asp phosphorelay in *Arabidopsis thaliana*. *Biosci. Biotechnol. Biochem.* **68**, 462–465.
- To, J.P.C., Haberer, G., Ferreira, F.J., Deruère, J., Mason, M.G., Schaller, G.E., Alonso, J.M., Ecker, J.R. and Kieber, J.J. (2004) Type-A ARRs are partially redundant negative regulators of cytokinin signaling in Arabidopsis. *Plant Cell*, **16**, 658–671.
- Tsai, Y.C., Weir, N., Hill, K., Zhang, W., Kim, H.J., Shiu, S.H., Schaller, E. and Kieber, J.J. (2012) Characterization of genes involved in cytokinin signaling and metabolism from rice. *Plant Physiol.* **158**, 1666–1684.
- Wang, W.-C., Lin, T.-C., Kieber, J. and Tsai, Y.-C. (2019) Response Regulators 9 and 10 negatively regulate salinity tolerance in rice. *Plant Cell Physiol.* **60**, 2549–2563.
- Wasilko, D.J., Edward Lee, S., Stutzman-Engwall, K.J., Reitz, B.A., Emmons, T.L., Mathis, K.J., Bienkowski, M.J., Tomasselli, A.G. and David Fischer, H. (2009) The titerless infected-cells preservation and scale-up (TIPS) method for large-scale production of NO-sensitive human soluble guanylate cyclase (sGC) from insect cells infected with recombinant baculovirus. *Protein Expr. Purif.* **65**, 122–132.
- Waterhouse, A.M., Procter, J.B., Martin, D.M.A., Clamp, M. and Barton, G.J. (2009) Jalview Version 2—a multiple sequence alignment editor and analysis workbench. *Bioinformatics*, **25**, 1189–1191.
- Waterhouse, R.M., Seppey, M., Simão, F.A., Manni, M., Ioannidis, P., Klioutchnikov, G., Kriventseva, E.V. and Zdobnov, E.M. (2017) BUSCO applications from quality assessments to gene prediction and phylogenomics. *Mol. Biol. Evol.* **35**, 543–548.
- Worthen, J.M., Yamburenko, M.V., Lim, J., Nimchuk, Z.L., Kieber, J.J. and Schaller, G.E. (2019) Type-B response regulators of rice play key roles in growth, development, and cytokinin signaling. *Development*, **146**, dev174870.
- Wybouw, B. and De Rybel, B. (2019) Cytokinin – a developing story. *Trends Plant Sci.* **24**, 177–185.
- Xia, L., Zou, D., Sang, J., Xu, X., Yin, H., Li, M., Wu, S., Hu, S., Hao, L. and Zhang, Z. (2017) Rice Expression Database (RED): an integrated RNA-Seq-derived gene expression database for rice. *J. Genet. Genomics*, **44**, 235–241.
- Xie, K., Zhang, J. and Yang, Y. (2014) Genome-wide prediction of highly specific guide RNA spacers for the CRISPR-Cas9 mediated genome editing in model plants and major crops. *Mol. Plant*, **7**, 923–926.
- Yeh, S.-Y., Chen, H.-W., Ng, C.-Y., Lin, C.-Y., Tseng, T.-H., Li, W.-H. and Ku, M.S.B. (2015) Down-regulation of cytokinin oxidase 2 expression increases tiller number and improves rice yield. *Rice*, **8**, 1–13.